V European Conference on Computational Fluid Dynamics
ECCOMAS CFD 2010
J. C. F. Pereira and A. Sequeira (Eds)
Lisbon, Portugal, 14–17 June 2010

HYBRID RANS/LES OF LOW REYNOLDS NUMBER ROUND IMPINGING JETS

Slawomir Kubacki[*], Erik Dick[†]

[*]Institute to Aeronautics and Applied Mechanics, Warsaw University of Technology,
Nowowiejska 24, 00-665 Warsaw, Poland
slawomir.kubacki@meil.pw.edu.pl

[†]Department of Flow, Heat and Combustion Mechanics, Ghent University,
Sint-Pietersnieuwstraat 41, 9000 Ghent, Belgium
erik.dick@ugent.be

Key words: Turbulence modelling, Hybrid RANS/LES model, Round impinging jet

Abstract. *Fluid flow and convective heat transfer predictions are presented for simulations of round impinging jets at nozzle-plate distances H/D=2, 6 and 13.5 and low and moderate Reynolds numbers Re=5000, 23000 with the newest k-ω model and two hybrid RANS/LES models. In RANS mode, both hybrid models reduce to the k-ω model. In LES mode, the first hybrid formulation (M1) uses the grid size in place of the turbulent length scale in the destruction term of the k-equation and in the definition of the eddy-viscosity. The second model (M2) uses the same k-equation as in model M1, but employs a Smagorinsky model for the subgrid viscosity in LES mode. The numerical results are compared with experimental data and fine grid dynamic Smagorinsky LES. At low nozzle-plate distance (the impingement plate is in the core of the jet), the turbulent kinetic energy is slightly overpredicted by the pure RANS k-ω model in the stagnation flow region. This leads to overprediction of the heat transfer rate along the impingement plate in the impact zone. At high nozzle-plate distance and low Reynolds number (impingement plate is in the mixed-out region of the jet), the turbulence mixing is underpredicted by RANS in the shear layer of the jet which gives a too high length of the jet core. This also results in overprediction of the heat transfer rate in the impingement zone due to too high shear stress at the wall. The hybrid RANS/LES models are able to overcome the deficiencies of the RANS model. At low and high nozzle-plate distances and moderate Reynolds number (Re=23000), both hybrid models are largely equivalent. However, at high nozzle-plate distance and low Reynolds number (Re=5000), the results of the first hybrid model (M1) are erroneous, similarly as the results of the pure RANS model, while the second hybrid model (M2) obtains very good agreement with the results of the dynamic Smagorinsky model.*

1 INTRODUCTION

Impinging jets are frequently used in industrial applications like tempering of glass, cooling of turbine blades or electronic equipment thanks to the high heat transfer rates which can be achieved in the stagnation flow region.

Close to the jet exit, roll-up vortices are formed due to Kelvin-Helmholtz instability. Further away from the jet exit, the roll-up vortices break up into smaller structures and impact the outer part of the wall jet. Secondary vortices are induced at the wall, as evidenced in LES studies [1,2]. The near-wall structures have a strong effect on the heat transfer between the wall and the fluid.

Since round impinging jets are challenging test cases due to the complexity of the turbulence dynamics, they are frequently used for validation of turbulence and subgrid scale models [3,4]. In the present work, the performance of two k-ω based hybrid RANS/LES models is studied for simulation of round impinging jets at different nozzle-plate distances and at two Reynolds numbers. We study also the performance of the pure k-ω model of Wilcox [5].

The flow physics and the heat transfer characteristics along the impingement plate have been extensively studied by experimental means [6-12]. Baughn and Shimizu [6], Baughn et al. [7] and Yan et al [8] performed measurements of the heat transfer rates along the plate for round impinging jets at Re=23000 for different distances between the nozzle exit and the impingement plate, ensuring that the flow is fully developed at the nozzle exit. Cooper et al. [9] performed measurements of the mean and fluctuating velocity profiles in the wall jet region for the same flow conditions as in [8] and additionally for Re=70000. Geers et al. [10] report measurements of the turbulent flow field for multiple round impinging jets and for a single impinging jet issuing from a long pipe of length L/D=72 with the distance between the jet exit and the impingement plate equal to H/D=2 and Re=23000. Colucci and Viscanta [11] demonstrate two peaks in the local Nusselt number profile for jet impingement at very low-nozzle plate distances (H/D=0.25 and 1). The inner peak (at R/D=0.5-0.8) was explained by thinning of the boundary layer due to flow acceleration while the outer (R/D=1.5-1.8) by transition from laminar to turbulent flow. The experiments of Liu and Sullivan [12] demonstrate that the vortex structures play a crucial role in enhancing or reducing the heat transfer rate in the near-wall region of the developing wall-jet.

The LES technique was employed to gain insight into the flow physics of round impinging jets at moderate and high Reynolds number by [1,2,11], among others. An accurate determination of the impinging jet heat transfer coefficient along the wall, at higher Reynolds number, is still very challenging for LES due to severe grid resolution requirements [1] and sensitivity to the subgrid scale model [2]. De Langhe et al. [14] used a hybrid RANS/LES model to study the heat transfer rate along the impingement plate for H/D=2 and 6, and Re=23000. Studies using DNS are limited to rather low Reynolds numbers [15].

We show results of simulations of round impinging jets with the two k-ω based hybrid RANS/LES models and the RANS k-ω model of Wilcox [5]. In RANS mode, both hybrid models reduce to the k-ω model. In LES mode, the destruction term in the k-equation is modified according to [16,17,18] in both hybrid models. Different formulations are used for the subgrid scale eddy viscosity in LES mode. In the first model, the turbulent length scale is replaced by the grid size based on the maximum of the three cell dimensions in a RANS type eddy-viscosity formula [18]. In the second model, the eddy-viscosity is computed with a Smagorinsky model [19] with the grid size defined by $\Delta_{LES}=(\Delta_x\Delta_y\Delta_z)^{1/3}$.

The numerical results are compared with experiments and LES reference data. We demonstrate that the first hybrid RANS/LES model is in error for simulation of a round impinging jet at low Reynolds number and large nozzle-plate distance. This is caused by too high dissipation in LES mode, which damps the small scale fluctuations in the shear layer of the jet. This behaviour is similar to that of the pure RANS k-ω model. As a result, the extent of the jet core region is too long, leading to overprediction of the heat transfer rate along the impingement plate. The second model does not have this deficiency since it uses a Smagorinsky model in LES mode. Both hybrid models give comparable results for simulation of round impinging jets at relatively high Reynolds number. For higher Reynolds number, the agreement of the predictions of the RANS k-ω model with the experiments is also much better.

2 HYBRID RANS/LES MODELS

Two hybrid RANS/LES formulations are studied, based on the k-ω model of Wilcox [5]. The transport equations read

$$\frac{Dk}{Dt} = \tau_{ij}\frac{\partial U_i}{\partial x_j} - \max\left(\beta^* k\omega, \frac{k^{3/2}}{C_{DES}\Delta}\right) + \frac{\partial}{\partial x_i}\left[\left(\nu + \sigma^*\frac{k}{\omega}\right)\frac{\partial k}{\partial x_i}\right], \tag{1}$$

$$\frac{D\omega}{Dt} = \alpha\frac{\omega}{k}\tau_{ij}\frac{\partial U_i}{\partial x_j} - \beta\omega^2 + \frac{\partial}{\partial x_i}\left[\left(\nu + \sigma\frac{k}{\omega}\right)\frac{\partial \omega}{\partial x_i}\right] + \frac{\sigma_d}{\omega}\frac{\partial k}{\partial x_i}\frac{\partial \omega}{\partial x_i}, \tag{2}$$

where ν is the kinematic molecular viscosity, k the turbulent kinetic energy and ω the specific dissipation rate. The components of the modelled stress tensor are $\tau_{ij}=2\nu_t S_{ij}-2/3k\delta_{ij}$ and the components of the rate of strain tensor are $S_{ij}=1/2(\partial U_i/\partial x_j+\partial U_j/\partial x_i)$. Following Kok [18], the model constant $C_{DES}=0.67$ and $\Delta=\max(\Delta_x, \Delta_y, \Delta_z)$, where Δ_x, Δ_y, Δ_z denote the distances between the cell faces in x, y and z directions. The remaining closure coefficients and relations are

$$\beta^* = 0.09, \quad \alpha = 0.52, \quad \beta = \beta_0 f_\beta, \quad \beta_0 = 0.0708 \quad \sigma = 0.5 \quad \sigma^* = 0.6 \quad \sigma_{do} = 0.125,$$

$$f_\beta = \frac{1+85\chi_\omega}{1+100\chi_\omega}, \quad \chi_\omega = \left|\frac{\Omega_{ij}\Omega_{jk}S_{ki}}{(\beta^*\omega)^3}\right|, \quad \sigma_d = \begin{cases} 0 & for \quad \dfrac{\partial k}{\partial x_j}\dfrac{\partial \omega}{\partial x_j} \le 0 \\ \sigma_{do} & for \quad \dfrac{\partial k}{\partial x_j}\dfrac{\partial \omega}{\partial x_j} > 0 \end{cases}$$

where $\Omega_{ij}=1/2(\partial U_i/\partial x_j-\partial U_j/\partial x_i)$.

In the first model discussed here (M1 model), the eddy-viscosity is defined by [18]:

$$\nu_t = \min\left(\frac{k}{\omega}, \beta^* C_{DES}\Delta\sqrt{k}\right). \tag{3}$$

In the second hybrid RANS/LES model (M2), the eddy-viscosity is defined by [19]:

$$\nu_t = \min\left(\frac{k}{\omega}, \left(C_s\Delta_{LES}\right)^2 S\right), \tag{4}$$

where $\Delta_{LES}=(\Delta_x\Delta_y\Delta_z)^{1/3}$, C_s is the Smagorinsky constant (here set to $C_s=0.1$) and $S=(2S_{ij}S_{ij})^{1/2}$ is the magnitude of the strain rate tensor.

Note that for simplicity, the RANS stress-limiter [5] is omitted in Eqs. (3) and (4), in the hybrid RANS/LES models. Our tests showed that the stress-limiter has only negligible effect on the results of the impinging jet flows with the hybrid RANS/LES models.

At the walls, the following conditions are used for k and ω:

$$k = 0, \quad \omega = \frac{u_\tau^2}{\nu} S_R, \tag{5}$$

where $S_R=\min[(200/k_s^+)^2, 6/(\beta_0(\Delta y^+)^2)]$, $\Delta y^+=\Delta y \cdot u_\tau/\nu$, $u_\tau=(\tau_w/\rho)^{1/2}$, $\tau_w=\mu \cdot S$ and k_s^+ is a dimensionless roughness height. As mentioned in [5], at smooth surfaces, the dimensionless roughness height k_s^+ is less than 5. Since the wall is assumed to be hydraulically smooth, the dimensionless roughness height was set here to $k_s^+ = 4$. The minimum function is used in the formula for S_R, so that the value of ω does not increase beyond its asymptotic value $\omega_0=6\nu/(\beta_0 \cdot (\Delta y)^2)$ in flow regions undergoing strong acceleration, where u_τ might grow very rapidly.

3 FLOW CONFIGURATION AND COMPUTATIONAL DETAILS

Fig. 1 shows a sketch of the computational domain together with the boundary conditions for simulation of round impinging jets at H/D=2 (unconfined jet). A similar computational domain was used for impinging jet simulations with nozzle-plate distance H/D=6. Figure 2 shows a sketch of a wall-jet electrode cell, together with the inlet section with the nozzle-plate distance H/D=13.5. In Figure 2, the part of the experimental set-up is indicated by the dashed border, which corresponds to the computational domain (confined impinging jet).

For the unconfined impinging jets (H/D=2 and 6), the inlet conditions correspond to that of fully developed pipe flow [6-9]. In order to reproduce the experimental conditions, the inlet profiles of velocity, k and ω were obtained from a precursor RANS simulation of the fully developed pipe flow using periodic boundary conditions. For the confined impinging jet (wall-jet reactor), fluid flow measurements were not acquired. For this case, axisymmetric flow simulations with the k-ω model were presented in Aerts et al. [20]. In [20], the flow in the inlet section (pipe A and B shown in Fig. 2a), together with the flow in the wall-jet reactor (indicated by the dashed line in Fig. 2a) was simulated. Fig 2b shows a comparison of the mean velocity profile obtained in [20] (denoted by reduced pipe diameter in Fig. 2b) with that obtained here from simulation of a fully developed pipe flow. The differences are small, so the flow at the jet exit can be treated as a fully developed one. In all simulations performed with the hybrid RANS/LES and LES models, a fully developed mean velocity profile has been imposed at the inlet to the computational domain. In addition, the RANS profiles of k and ω have been used to generate fluctuations at the inlet to the computational domain using the vortex method of Fluent.

The computational grids for the hybrid RANS/LES and LES models consist of unstructured (at R/D<0.5) and block-structured (at R/D>0.5) parts. The grid points have been clustered towards the walls, in order to fulfil the condition $y^+<3$, and also in the radial direction in the shear layer of the jet (at R/D=0.5).

Extremely fine grids have been generated for the RANS simulations The grid points have been clustered close to the impingement plate, symmetry axis, jet exit and towards the edge of the nozzle (in the free shear layer), and along the impingement plate, $y^+<0.5$. It was verified that with RANS, grid independent solutions have been obtained.

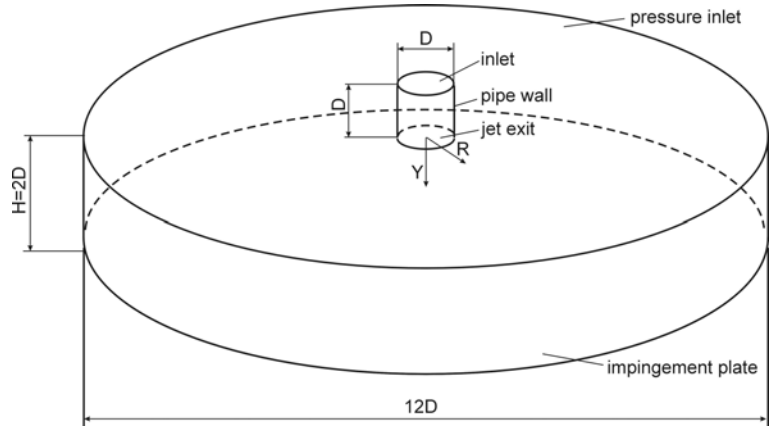

Figure 1: Computational domain, boundary conditions and coordinate system for simulation of the round impinging jet at H/D=2.

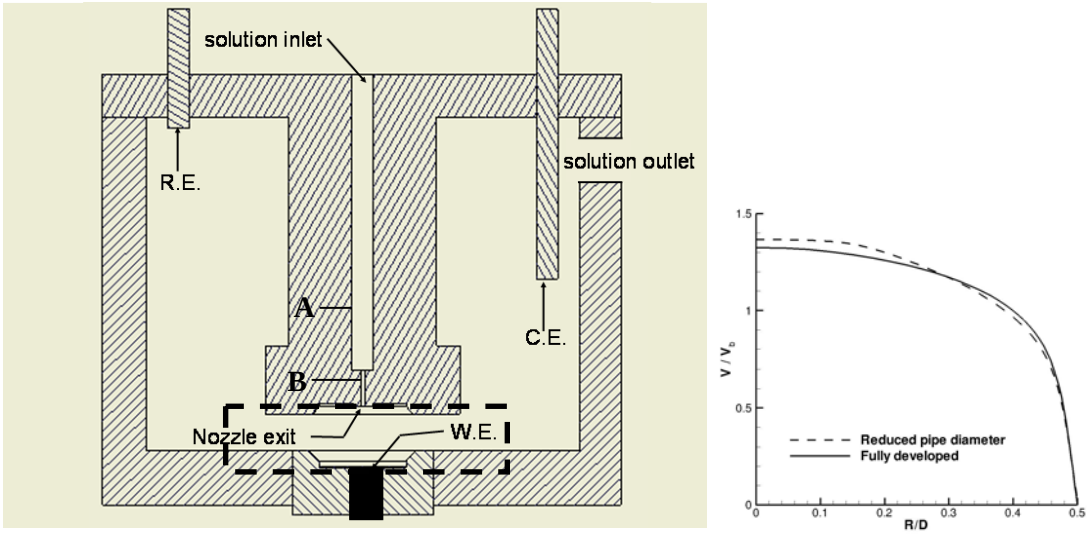

Figure 2: (left) Cross section through the wall-jet electrode cell, (right) comparison of the mean velocity profiles at the jet exit.

The computations have been performed with the Fluent code, version 12. The transport equations were implemented with the used-defined scalar functionality. The bounded central differencing scheme was applied to the convective terms in the momentum equations and the second order upwind scheme to the convective terms in the energy, k- and ω-equations.

The heat transfer is modelled with the energy equation with the gradient diffusion hypothesis for the modelled heat flux:

$$\overline{u_i' \vartheta'} = -\frac{\nu_t}{\mathrm{Pr}_t} \frac{\partial T}{\partial x_i}, \tag{6}$$

where u_i' denote the fluctuating velocity component while T and ϑ' denote the mean and fluctuating temperatures, and Pr_t is the turbulent Prandtl number (Pr_t=0.85).

The heat transfer rates along the impingement plate are analysed with the Nusselt number

$$Nu = \frac{-\partial T / \partial y|_W D}{T_W - T_{inl}}, \tag{7}$$

where D is the jet nozzle diameter. A constant value of the temperature T_W=310K was imposed on the impingement plate. The inlet temperature was set to T_{inl}=300K. The remaining walls are adiabatic. For the hybrid simulations and the LES, the Nusselt number profiles were averaged in time and in the azimuthal direction.

4 RESULTS

4.1 Mean and fluctuating velocities for unconfined impinging jet

Figure 3 shows profiles of the mean velocity components obtained with the k-ω RANS and the two hybrid RANS/LES models, and the comparison with the experimental data of Cooper et al. [9]. The data are normalized with the bulk velocity V_b at the jet exit. For the hybrid models, all velocity profiles were averaged in time and in azimuthal direction. First of all, we see that a very good agreement is obtained between predictions using RANS and the experimental data. The good quality of the RANS is due to the stress-limiter [5], which controls the turbulent shear stress in the stagnation flow region.

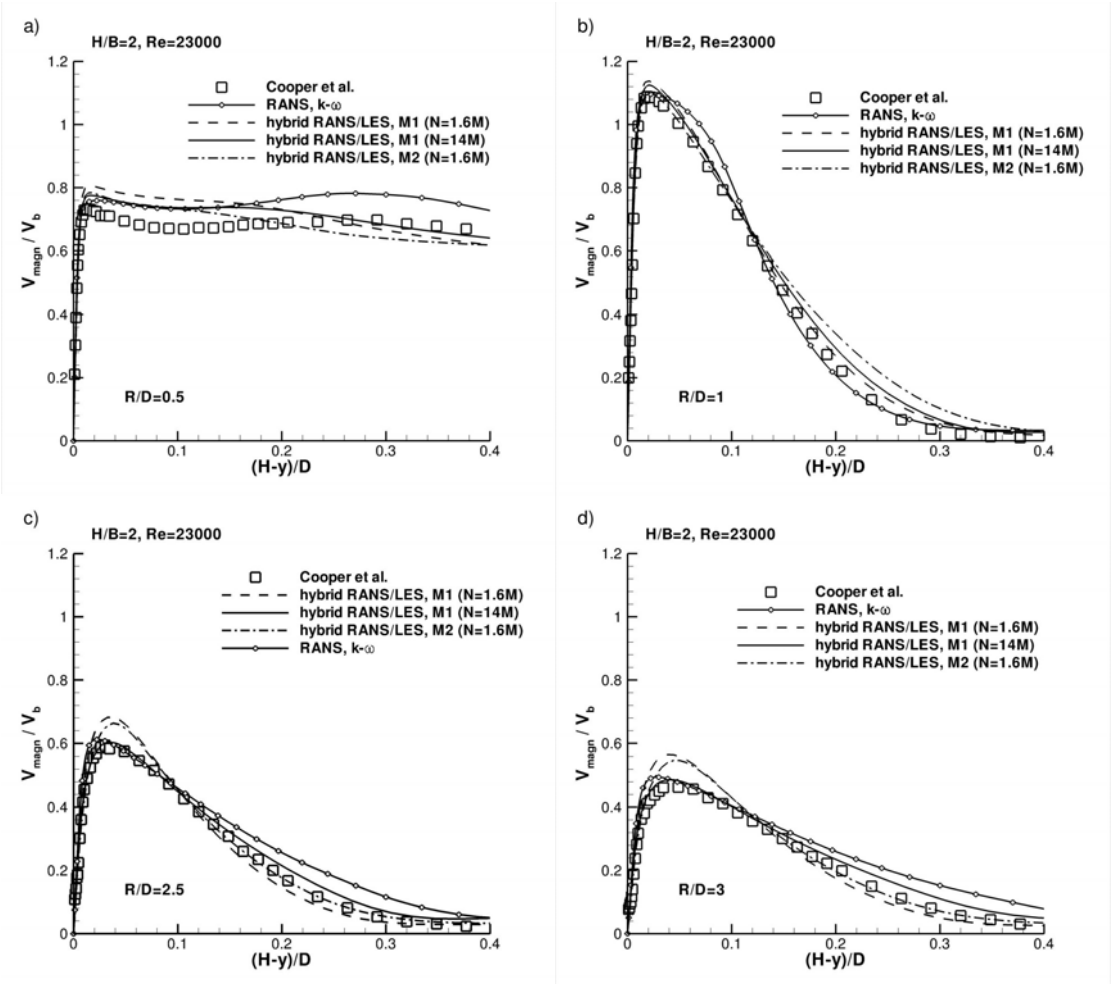

Figure 3: Mean velocity magnitude along lines perpendicular to the impingement plate for H/D=2, Re=23000, at distances from the jet axis a) R/D=0.5, b) R/D=1, c) R/D=2.5 and d) R/D=3.

The two coarse grid results obtained with the hybrid RANS/LES models (M1 and M2 with N=1.6 million grid cells) are in good agreement with the experiments at radial distances R/D=0.5 and 1 (Fig. 3a and 3b). On the coarse grids, both hybrid RANS/LES models return somewhat higher peaks of the mean velocity magnitude at radial distances R/D=2.5 and 3 (Fig. 3c and 3d). This is due to insufficient grid resolution in azimuthal direction, so that the break-up of the vortices cannot be completely captured there. The results obtained on the fine grid (14 million cells) with the M1 hybrid RANS/LES model are in good agreement with the experimental data. It should be stressed that even on the coarse grid (1.6M), some important flow features like the decay of the mean velocity in the viscous sublayer and the spreading of the mean velocity into the free stream are well reproduced with the hybrid RANS/LES models.

The profiles of the radial and wall-normal fluctuating velocity components are shown in Figures 4 and 5. The RANS fluctuating velocity components are computed as $(2k/3)^{1/2}$. For the hybrid RANS/LES models, resolved fluctuations are shown. The numerical results are compared with experimental data of Cooper et al. [9] and Geers et al. [10]. One should note the differences between both experimental data sets (Figs. 4a and 4b, 5a and 5b).

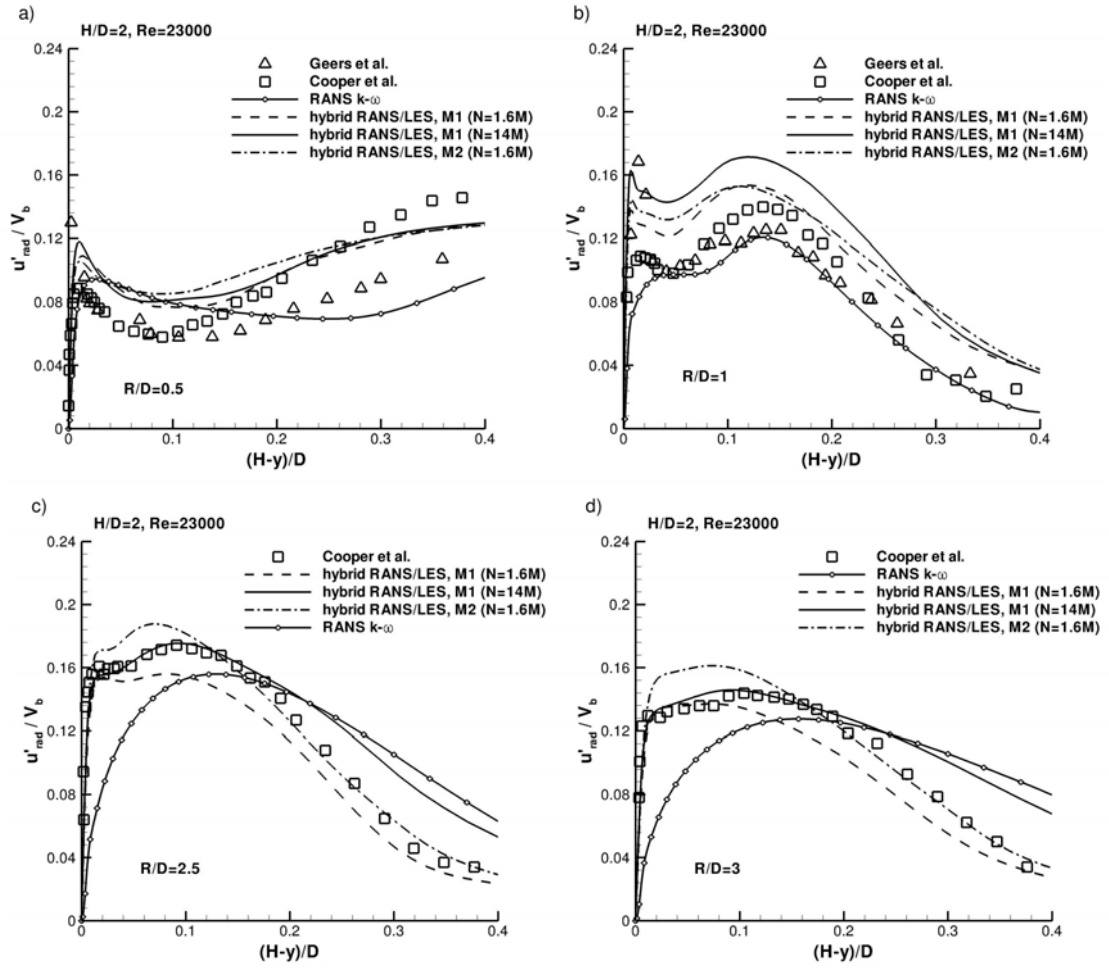

Figure 4: Radial fluctuating velocity component along lines perpendicular to the impingement plate for H/D=2, Re=23000, at distances from the jet axis a) R/D=0.5, b) R/D=1, c) R/D=2.5 and d) R/D=3.

As shown in Figure 5a and 5b, the wall-normal fluctuating component predicted by RANS is higher than the data in the near-wall region ((H-y)/D<0.1). It means that the turbulent kinetic energy is overpredicted there. This is a well known deficiency of eddy-viscosity RANS models in an impingement zone due to the isotropic representation of the turbulence. Note that overprediction of the turbulent kinetic energy does not lead to erroneous mean velocity profiles (Fig. 3a and 3b). The radial fluctuations by the hybrid RANS/LES models agree fairly well with the experimental data at R/D=0.5, 2.5 and 3 (Fig. 4a, 4c and 4d). The correspondence between experiment and computations is somewhat less at R/D=1 (Fig. 4b). This is however the region of strong flow acceleration. So, the overprediction of the radial fluctuating velocity component by the hybrid models might be explained by shortcoming of the eddy-viscosity based models [4]. There are no big differences between coarse and fine grid results. The correspondence between the results of the hybrid models and the experiments seems to be somewhat less for the wall-normal fluctuations (Fig. 5), but one has to take into account significant differences between the two experimental data sets. There is also more sensitivity to grid resolution.

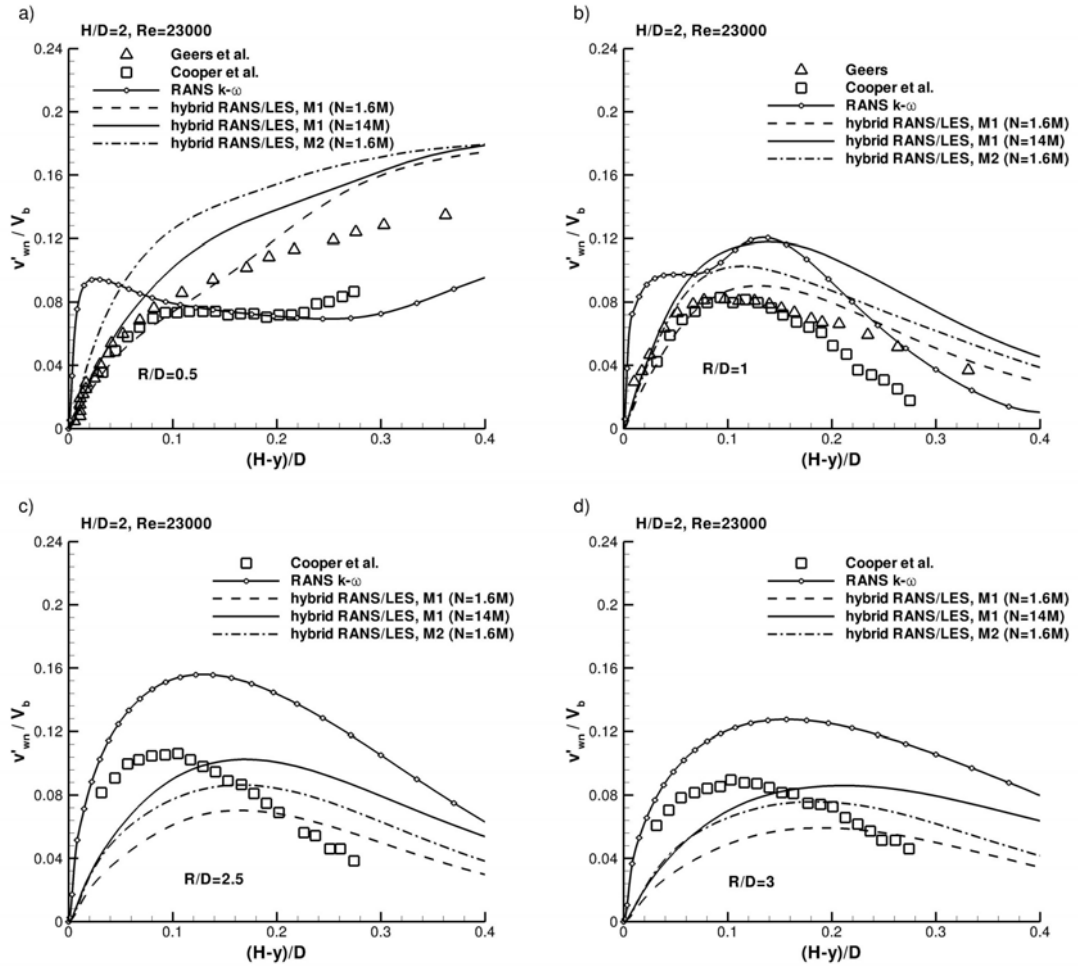

Figure 5: Wall-normal fluctuating velocity component along lines perpendicular to the impingement plate for H/D=2, Re=23000, at distances from jet axis a) R/D=0.5, b) R/D=1, c) R/D=2.5 and d) R/D=3.

Close to the wall ((H-y)/D<0.1) the agreement between measurements and computations with the hybrid models is very good for R/D =0.5 and R/D=1 (Fig. 5a and 5b). For R/D>1, the agreement is less and improvement is obtained by grid refinement.

This shows that an enormous grid resolution is required if one wants to capture the break-up of the near-wall vortices accurately. Note that similar differences were observed by Lodato et al. [4] between results of LES and the experimental data of the radial and wall-normal fluctuations. In [4], the difficulty in reproducing the correct levels of the radial and wall-normal fluctuating velocity components was explained by shortcomings of the subgrid scale models. We, however, think that lack of resolution for larger distances from the jet axis is a more plausible cause for the differences.

4.2 Mean and fluctuating velocities for confined impinging jet

Figure 6 shows the mean and fluctuating velocity profiles along the symmetry axis for the simulation of the confined round impinging jet with the nozzle-plate distance H/D=13.5 and Re=5000. The nozzle exit is placed at y/D=0 and the impingement plate corresponds to y/D=13.5. The mean and fluctuating velocities are normalized by the bulk velocity V_b at the jet exit. Experimental data of velocity are not available for this test case. We use here as reference the results obtained from LES with the dynamic Smagorinsky model on a grid of 7M cells. These results are reliable because the Reynolds number of the flow is low. All hybrid RANS/LES model simulations have been performed on a grid of 2M cells. As shown in Figure 6, the pure RANS k-ω model predicts too slow decay of the mean velocity profile along the jet axis. This is due to underprediction of the turbulence mixing in the shear layer of the jet, which is a known deficiency of an eddy viscosity type RANS model [21].

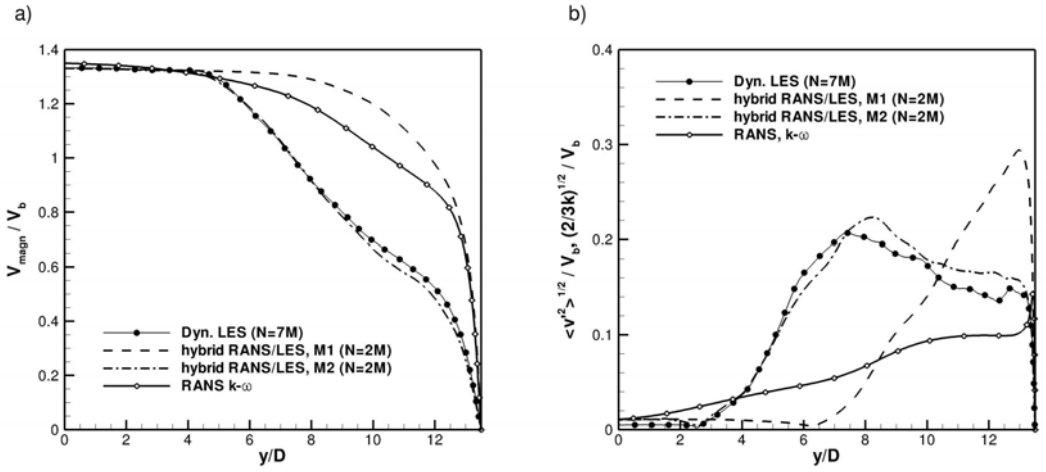

Figure 6: Profiles of a) mean velocity magnitude and b) axial fluctuating velocity component (LES and hybrid models: resolved fluctuations) along the jet axis for confined round impinging jet simulation at Re=5000.

The M1 hybrid model predicts a similar erroneous mean velocity profile at the symmetry axis. Figure 6b shows that with the M1 model, the fluctuating velocity component starts to rise too far downstream from the nozzle exit (y/D=7), with respect to the LES result (y/D=3). This means that the M1 model produces too much dissipation in the shear layer of the jet, so that the LES-like eddies cannot form. The deficiency of the M1 model is repaired with the second hybrid model M2, where in LES mode the eddy-viscosity is computed with the Smagorinsky model, with the grid length scale given by $\Delta_{LES}=(\Delta_x\Delta_y\Delta_z)^{1/3}$ and with the model constant set to $C_s=0.1$ (Eq. 4). With the M2 hybrid model, both the mean and fluctuating velocity profiles are close to the profiles obtained with the dynamic LES model.

4.3 Heat transfer

Figure 7a shows the Nusselt number profile along the impingement plate for simulation of the impinging jet flow at H/D=2 and Re=23000. The numerical results are compared with experimental data of Baughn and Shimizu [6], Baughn et al. [7] and Yan et al. [8]. RANS overpredicts the stagnation point Nusselt number. This is due to slight overprediction of the turbulent kinetic energy in the near-wall region of the impact zone. At R/D>1.5, RANS results show too strong decay of the Nusselt number profile compared to the experiment. For this case, similar results have been obtained with the k-ω model by Jaramillo et al. [3]. So, here, the k-ω model gives a somewhat too strong damping of the turbulent kinetic energy in the near-wall region away from the jet axis. The dotted line shows the heat transfer rate obtained for turbulent flow simulation but setting to zero the turbulent diffusivity in the energy equation. This result demonstrates that the turbulent diffusion does not play a crucial role in the enhancement of the heat transfer in the stagnation flow region (R/D<1.2) and that it becomes more relevant at larger distance from the symmetry axis (R/D>1.2). Such a transitional behaviour of the Nusselt number profile is difficult to reproduce with RANS. In the impingement zone, the heat transfer rates obtained by the hybrid models M1 and M2 on the coarse grid (N=1.6M) are in good agreement with the measured heat transfer rates. The secondary peak is not captured. At larger radial locations (R/D>3.5), the Nusselt number profile by the hybrid models collapse well with the Nusselt number profile predicted by the pure k-ω RANS model. There is slight improvement in the heat transfer rates at R/D=2 if the hybrid M1 model is used on a fine grid (14M). The peak value of the Nusselt number is not as strong as in the experiment. The cause is that even on a fine grid, most of the thermal boundary layer resides in the RANS mode of the hybrid RANS/LES model. Remark that also the LES results obtained by [2] show too strong decay of the Nusselt number profile at larger distance from the jet axis. It shows that with LES, extremely fine grids have to be used in order to correctly reproduce the heat transfer rates at larger distances from the symmetry axis.

Figure 7b shows the heat transfer rates predicted by RANS and by the hybrid RANS/LES models for round impinging jet simulation at H/D=6 and Re=23000. The computations were performed on the basic grid with 1.6M cells. For this case, the heat transfer rates predicted by the k-ω RANS model are in quite good agreement with the experimental data. Similarly to the previously discussed results (H/D=2, Re=23000), the heat transfer rates are somewhat underpredicted by RANS at R/D>3. Both hybrid models give similar results. The stagnation point Nusselt number is slightly underpredicted, but the decay of the Nusselt number profile at 0.5<R/D<1.5 is in good agreement with the experimental data. At R/D>5 the Nusselt number profiles produced by the hybrid models converge to the Nusselt number profile obtained with the k-ω RANS model. For 1.5<R/D<5, there is underprediction of the heat transfer, similar as in the previous cases. Again, this underprediction is caused by lack of resolution.

Figure 8 shows the heat transfer rates predicted by RANS and by the hybrid RANS/LES models for the confined impinging jet simulation with H/D=13.5 and Re=5000. As demonstrated in Figure 6, the decay of the mean velocity profile along the jet axis is incorrectly predicted by both the RANS and M1 hybrid models. This error has big consequences for the heat transfer rate prediction in the impact zone. Both the RANS and M1 hybrid models predict the stagnation point Nusselt number about 40% higher than the Nusselt number obtained with the dynamic Smagorinsky model. For comparison, the stagnation point Nusselt number calculated from a correlation of Lee and Lee [22] is also shown in Figure 8. Remark that the correlation is based on measurements performed for unconfined round impinging jets (in contrast to the

confined jet studied here), with nozzle-plate distances varying from H/D=2 to 10 (here H/D=13.5). The overprediction of the heat transfer by the RANS and M1 hybrid models is due to too high shear stress in the impingement zone (see Fig. 6a). In contrast, the M2 model gives heat transfer rates which agree well with the heat transfer rates from the LES. Further away from the stagnation point region (R/D>2), all models give very similar results.

This test case demonstrates the deficiencies of the pure RANS and the M1 hybrid models. As mentioned, RANS is in error due to underprediction of the turbulence mixing in the shear layer of the jet, while the hybrid M1 models returns too high dissipation in the shear layer of the jet which results in damping of the resolved fluctuations in the shear layer of the jet.

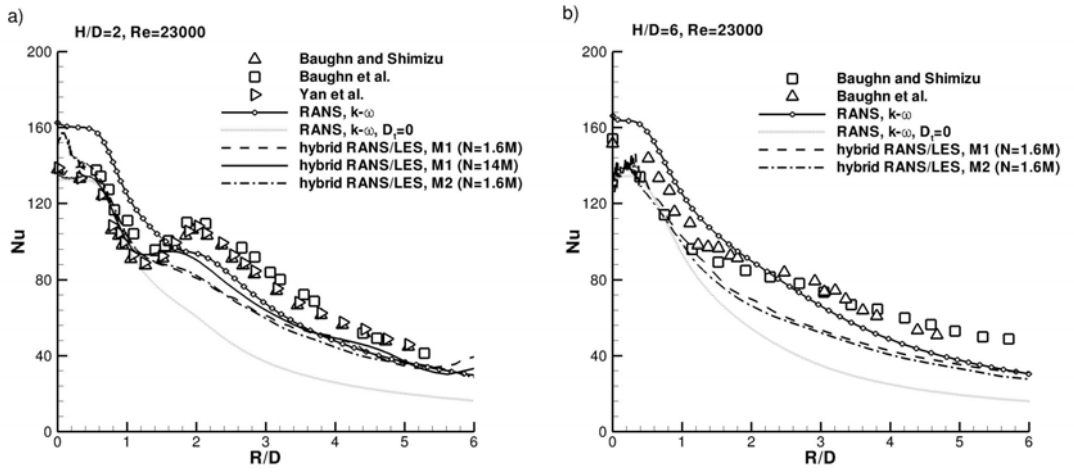

Figure 7: Nusselt number profile along the impingement plate for a) H/D=2 ,b) H/D=6 and Re=23000.

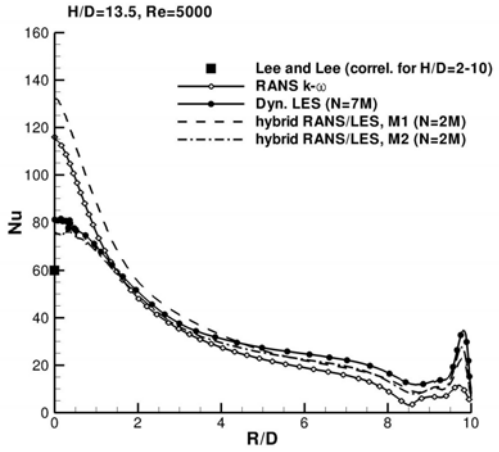

Figure 8: Nusselt number profile along the impingement plate for H/D=13.5, Re=5000.

5 SUMMARY

Results of simulations of round impinging jets at low and high nozzle-plate distances (H/D=2-13.5) and at low and moderate Reynolds numbers (Re=5000 and 23000) were presented using the k-ω RANS and two hybrid RANS/LES k-ω based models. The mean and fluctuating velocities were analyzed in the wall-jet region. Particular attention went to the ability of the k-ω RANS and hybrid RANS/LES models to reproduce the heat transfer coefficient along the impingement plate.

At low nozzle-plate distance (H/D=2), the k-ω RANS model predicts the stagnation point Nusselt number higher than the measured one. This is due to slight overprediction of the turbulent kinetic energy in the near-wall region in the impingement zone by the k-ω RANS model. At high nozzle-plate distance and low Reynolds number, the k-ω RANS model has a tendency to underpredict the turbulence mixing in the shear-layer of the jet. This also leads to overprediction of the heat transfer rates in the stagnation flow region.

The deficiencies of the RANS model can be cured by hybrid RANS/LES models if the grids are fine enough to resolve the break-up of the ring vortices in the shear layer of the jet and the formation of the secondary vortices in the near-wall region. Two hybrid models have been studied. Model M1 uses a subgrid eddy viscosity of RANS type, with reduced length scale. Model M2 uses a subgrid viscosity of Smagorinsky type. Both hybrid models are able to reproduce the correct heat transfer rates in the stagnation flow region for Re=23000. Further away from the jet axis, the heat transfer rates obtained with the hybrid models converge to the heat transfer rates obtained with the pure RANS model. Extremely high grid density is required for impinging jet flow simulation with the hybrid models at low nozzle-plate distance (H/D=2), in order to fully capture the transition from the stagnation region flow to the developing wall-jet flow. This is due to necessity to resolve the break-down of the near-wall vortices in the developing wall-jet region, which has a strong impact on the heat transfer rates along the impingement plate. For H/D=2 and Re=23000, the secondary peak in the Nusselt number profile was not reproduced by the hybrid models on the coarse grids (1.6M) and the result was somewhat better for the hybrid M1 model simulation on the fine grid (14M). The grid resolution requirements are also high for the case H/D=6 and Re=23000. Here, lack of grid resolution caused too strong decay of the Nusselt number profile with the hybrid models at $1.5<R/D<5$.

One has to be careful with hybrid RANS/LES models for simulation of round impinging jets at low Reynolds number. The M1 model was found to dissipate too much in the shear layer of the jet, so that the jet spreading rate was highly underpredicted. As a result, the heat transfer rates were overpredicted in the impact zone of the jet. The M2 model does not have this deficiency. For a low Reynolds number flow, the heat transfer rates predicted with the M2 model were similar to those obtained with the dynamic LES model.

ACKNOWLEDEMENT

The authors acknowledge the support from the research project ‘Novel Multiscale Approach to Transport Phenomena in Electrochemical Processes’ (IWT, contract: MuTEch SBO 040092).

REFERENCES

[1] M. Olsson and L. Fuchs, Large eddy simulations of a forced semiconfined circular impinging jet. *Phys. Fluids*, **10**, 476-486 (1998)

[2] M. Hadziabdic and K. Hanjalic, Vortical structures and heat transfer in a round impinging jet. *J. Fluid Mech.,* **596**, 221-260 (2008)

[3] J.E. Jaramillo, C.D. Perez-Segarra, I. Rodriguez and A. Oliva, Numerical study of plane and round impinging jets using RANS models. *Numer. Heat Transfer*, *Part B,* **54**, 213-237 (2008).

[4] G. Lodato, L. Vervisch and P. Domingo, A compressible wall-adapting similarity mixed model for large-eddy simulation of impinging round jet. *Phys. Fluids,* **21**, 1-21 (2009).

[5] D.C., Wilcox, Formulation of the k-ω turbulence model revisited. *AIAA Journal,* **46,** 2823-2837 (2008)

[6] J.W. Baughn and S. Shimizu, Heat transfer measurements from a surface with uniform heat flux and an impinging jet. *J. of Heat Transfer,* **111**, 1096-1098 (1989)

[7] J.W. Baughn, A.E. Hechanova and X. Yan, An experimental study of entrainment effects on the heat transfer from a flat surface to a heated circular impinging jet. *J. of Heat Transfer,* **113**, 1023-1025 (1991)

[8] X. Yan, J.W. Baughn and M. Mesbah, The effect of Reynolds number on the heat transfer distribution from a flat plate to an impinging jet. *ASME HTD,* **226**, 1-7 (1992)

[9] D. Cooper, D.C. Jackson, B.E. Launder and G.X. Liao, Impinging jet studies for turbulence model assessment-I. Flow-field experiments. *Int. J. Heat Mass Transfer,* **36**, 2675-2684 (1993)

[10] L.F.G. Geers, M.J. Tummers and K. Hanjalic, Experimental investigation of impinging jet arrays. *Exp. in Fluids,* **36**, 946-958 (2004)

[11] D.W. Colucci and R. Viscanta, Effect of nozzle geometry on local convective heat transfer to a confined impinging air jet. *Exp. Thermal Fluid Science,* **13**, 71-80 (1996)

[12] T. Liu and J.P. Sullivan, Heat transfer and flow structures in an excited circular jet. *Int. J. Heat mass Transfer,* **39**, 3695-3706 (1996)

[13] M. Olsson and L. Fuchs, Large eddy simulations of a forced semiconfined circular impinging jet, *Phys. Fluids,* **10**, 476-486 (1998)

[14] C. De Langhe, J. Bigda, K. Lodefier and E. Dick, One-equation RG hybrid RANS/LES computation of a turbulent impinging jet, *J. of Turbulence,* **9**, 1-19 (2008)

[15] M. Tsubokura, T. Kobayashi, N. Taniguchi and W.P. Jones, A numerical study on the eddy structures of impinging jets exited at the inlet, *Int. J. Heat Fluid Flow,* **24**, 500-511 (2003)

[16] M. Strelets, Detached eddy simulation of massively separated flows, *AIAA Paper* 2001-0879 (2001)

[17] L. Davidson and S.H. Peng, Hybrid LES-RANS modelling: a one-equation SGS model combined with a k-ω model for predicting recirculating flows, *Int. J. Numer. Meth. Fluids,* **43**, 1003-1018 (2003)

[18] J.C. Kok, H. Dol, H. Oskam and H. van der Ven, Extra-large eddy simulation of massively separated flows, *AIAA Paper* 2004-0264 (2004)

[19] P. Batten, U. Goldberg and S. Chakravarthy, Interfacing statistical turbulence closures with large-eddy simulation, *AIAA Journal,* **42**, 485-492 (2004)

[20] T. Aerts, I. De Graeve, G. Nelissen, J. Deconinck, S. Kubacki, E. Dick and H. Terryn, Experimental study and modelling of anodizing of aluminium in wall-jet electrode set-up in laminar and turbulent regime, *Corrosion Science,* **51**, 1482-1489 (2009)

[21] N.J. Georgiadis, D.A. Yoder and W.A. Engblom, Evaluation of modified two-equation turbulence models for jet flow predictions, *AIAA Journal,* **44**, 3107-3114 (2006)

[22] J. Lee and S.-J. Lee, Stagnation region heat transfer of a turbulent axisymmetric jet impingement, *Exp. Heat Transfer,* **12**, 137-156 (1998)